Chemical Engineering Science. Vol. 40, No. 12, pp. 2249–2259, 1985.
Printed in Great Britain.

0009–2509/85 $3.00 + 0.00
Pergamon Press Ltd.

ANALYSIS OF NON-EXPLOSIVE BUBBLE GROWTH WITHIN A SUPERHEATED LIQUID DROPLET SUSPENDED IN AN IMMISCIBLE LIQUID†

C. T. AVEDISIAN‡ and K. SURESH§
Sibley School of Mechanical and Aerospace Engineering, Cornell University, Ithaca, NY 14853, U.S.A.

(*Received* 16 *November* 1984)

Abstract—Bubble growth within a volatile droplet (liquid 1) at its superheat limit suspended in an immiscible nonvolatile field liquid (liquid 2) is analysed by solving the coupled energy and momentum equations for the temperature fields in liquids 1 and 2. A numerical solution is presented for a two-phase droplet modelled as a vapour bubble growing from the centre of liquid 1. It is shown that when the properties of liquids 1 and 2 are appreciably different, the bubble growth rate can experience a significant increase or decrease when the thermal boundary layer extends into liquid 2. The present calculations are also compared with available data and the agreement is reasonable.

1. INTRODUCTION

An understanding of bubble growth within a superheated liquid droplet is important in many applications related to mixing of immiscible liquids. These include ln g spills on water, preparation of emulsified liquids, fuel coolant interactions in postulated nuclear reactor accidents, and three-phase heat exchangers. In these applications a volatile liquid is often dispersed in another nonvolatile stagnant liquid in the form of droplets. Subsequent heating of the field liquid can lead to substantial superheating of the dispersed droplets, followed by homogeneous nucleation, and finally bubble growth. Our understanding of predictive methods for the initial conditions for growth defined by homogeneous nucleation is rather complete. Things are different for the bubble growth problem.

Previous work has focused on the effect of the droplet on the flow and heat transfer in the external field liquid, with a concomitant neglect of processes within the droplet. For example, previous analyses have used one or more of the following approximations: (1) quasi-steady heat transfer in the field liquid, (2) assuming the droplet to be a rigid sphere, (3) negligible temperature gradients within the droplet, (4) neglecting the finite volume of the vaporizing liquid and in effect treating the problem as though a bubble were growing in an infinite medium, and (5) treating part (or all) of the evaporating boundary as planar [1–8]. The first three assumptions are reasonable for high Péclet number (based on a droplet in a stream moving at U_∞) relative to the Jakob number—in particular $Pe \gg Ja^3$ (this fact may be shown by nondimensionalizing the energy equation and boundary conditions appropriate to this problem, followed by a simple ordering of terms). This condition is satisfied in many experiments involving droplets evaporating at low superheats (i.e. far from their superheat limits) in a moving stream (e.g. [1–6]).

The present work considers the limit of low Péclet number and a droplet at its homogeneous nucleation limit—$Pe \to 0$ while $Ja \sim 1$–100. In this limit the evolution of the thermal boundary layer, from its movement in the droplet out into liquid 2 (Fig. 1), must be determined. Neither the thin thermal boundary layer nor quasi-steady assumptions are universally valid. Unsteady heat transfer in both the droplet and ambient liquid must then be included in the analysis. The dynamics of growth (i.e. pressure field) may be effected from the beginning by the finite mass of vaporizing liquid (through its effect on the momentum equation) and this is included in the present study. While both the temperature field in the droplet and the bubble growth rate may be similar to growth in an infinite medium during the period in which the boundary layer resides in the droplet [Fig. 1(a)], the problem is fundamentally different from bubble growth in an infinite medium because of eventual penetration of the thermal boundary layer into liquid 2 [Fig. 1(b)]. The temperature field then becomes a two-domain problem.

This paper presents a solution to the equations governing the dynamics and heat transfer of bubble growth within a volatile liquid droplet when the droplet is at its limit of superheat in a comparatively stagnant, initially isothermal, nonvolatile field liquid. We adopt several assumptions commonly made in studies of bubble growth in infinite media (e.g. [9]—constant properties, incompressible liquids, Newtonian fluids no frictional heating, etc.). We also assume: (1) liquids 1 and 2 are mutually immiscible, (2) the droplet/field liquid system is initially at a uniform temperature T_0 which corresponds to the homogeneous nucleation limit of liquid 1 at pressure P_0, (3) a bubble grows from the centre of liquid 1

†Part of this paper was presented at the 22nd National Heat Transfer Conference, Niagara Falls, 5–8 August 1984.
‡To whom correspondence should be addressed.
§Present address: Alcohol Energy Systems, 1050H Duane Avenue, Sunnyvale, CA 94086, U.S.A.

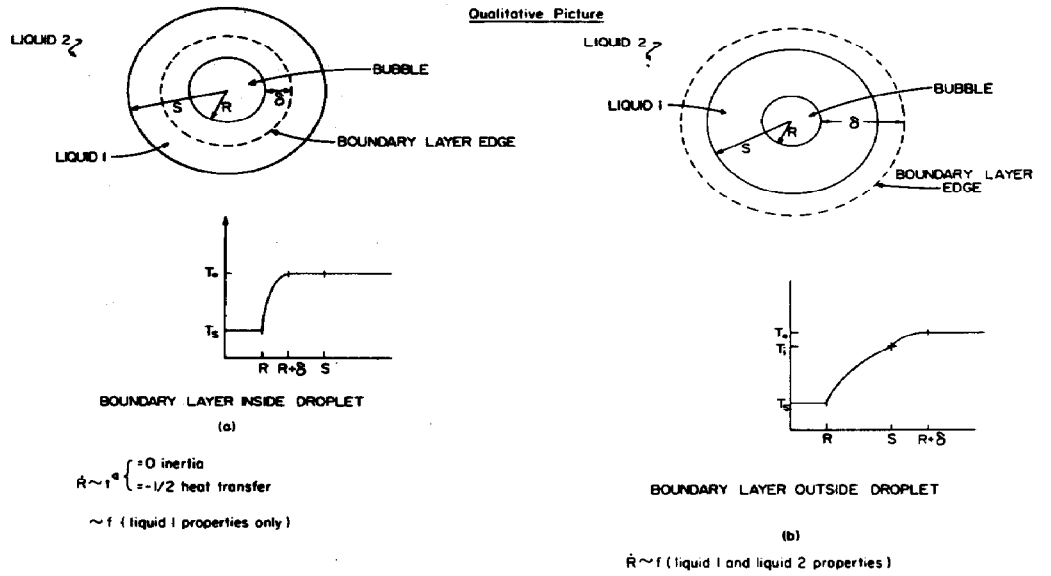

Fig. 1. Schematic illustration of bubble growth in a droplet suspended in an immiscible liquid. (a) Early stage where thermal boundary layer (δ) is within the droplet; (b) later stage when boundary layer extends into liquid 2.

[Fig. 2(a)] and its centre does not move, and (4) bubble oscillations and effects of evaporation-induced instabilities characteristic of vapour explosions [10, 11] are not considered (the present analysis thus applies to ambient pressures high enough that such effects are absent—$P_r > 0.2$–0.4 for most organic liquids [8]).

The second assumption provides a direct relation between vapour pressure and ambient temperature (no dissolved gas effects), and it also implies that the bubble will reside entirely within the droplet during its growth (the case in which a bubble leaves the droplet sometime during growth is treated in Ref. 6). In an initially isothermal droplet the location of the critical size nucleus defined by homogeneous nucleation is indeterminate in that there are no constraints with which to determine its position within the droplet (for a nonisothermal droplet, however, it would be reasonable to assume the nucleus forms at the hottest location). The simplest case was, therefore, treated first—a bubble in the geometric centre of a droplet [Fig. 2(a)]. For an eccentrically located initial bubble—Fig. 2(b)—(i.e. initially nonisothermal droplet), experimental evidence (e.g. [2]) has shown that when as little as 1 % (by weight) of liquid has vaporized for many organic droplets, liquid surrounding the bubble essentially exists in the form of a thin film (due to the large liquid to vapour density ratio). Eccentricity effects will then be unimportant. Thermal resistance in this film may not, however, generally be neglected. Discrepancies between calculated and measured growth rates caused by assuming a concentric bubble configuration [Fig. 2(a)] vs. an eccentric location [Fig. 2(b)] might, most likely, be experienced during the early stages of growth when the thickness of the liquid film surrounding the bubble is still significant (in the

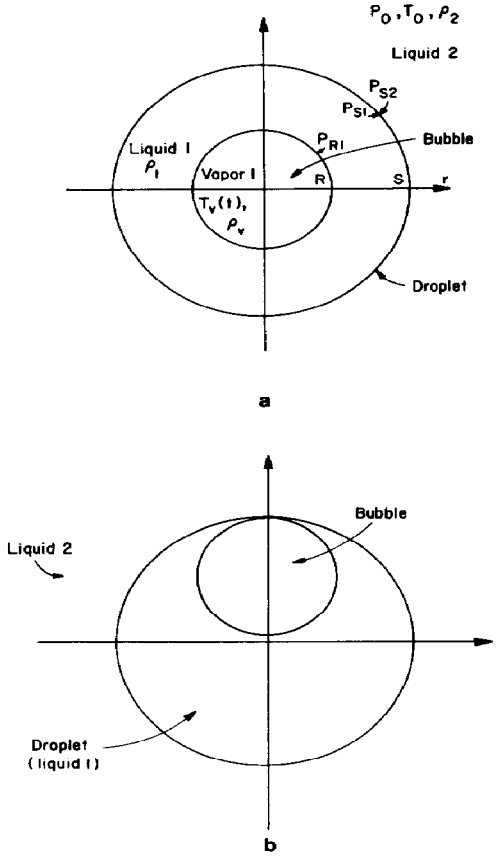

Fig. 2. Geometric model for bubble growth in a liquid droplet. (a) Model used in present analysis (pressures correspond to values at indicated interfaces); (b) eccentric bubble geometry for initially nonisothermal droplet such that initial bubble appears at liquid 1/liquid 2 interface.

limit $R_0 \to 0$ this film thickness would simply be S_0). However, the source of any discrepancies seems to point to experimental uncertainty and other effects not included in the present analysis as mentioned in Section 4. The neglect of buoyancy and other possible causes of motion of the growing bubble (there will be no surface tension driven or nonradial flow in this spherically symmetric system) is certainly valid during the early stages of growth due to the small initial bubble size—typically 10^{-7} cm. Buoyancy effects on heat transfer to the internal bubble could conceivably become important sometime during growth. However, in view of the comparatively large volume occupied by the internal bubble early in its growth, we do not include this complicating effect in the present analysis.

2. FORMULATION

Consider a vapour bubble growing from the centre of liquid 1 which in turn is suspended in liquid 2 [Fig. 2(a)]. The velocity, pressure and temperature fields in the two liquids are governed by the solution to the following set of continuity, momentum and energy equations for liquids 1 and 2:

$$\frac{1}{r^2}\frac{\partial}{\partial r}(r^2 v_i) = 0$$

$$\frac{\partial v_i}{\partial t} + v_i\frac{\partial v_i}{\partial r} = -\frac{1}{\rho_i}\frac{\partial P_i}{\partial r} + \nu_i\left[\frac{1}{r^2}\frac{\partial}{\partial r}\left(r^2\frac{\partial v_i}{\partial r}\right) - \frac{2v_i}{r^2}\right]$$

$$\frac{\partial T_i}{\partial t} + v_i\frac{\partial T_i}{\partial r} = \alpha_i\frac{1}{r^2}\frac{\partial}{\partial r}\left(r^2\frac{\partial T_i}{\partial r}\right)$$

and $$P_v = f(T_v)$$

where $i = 1$ and 2.

The boundary and initial conditions are the following:

$$T_1(r,0) = T_2(r,0) = T_0 \quad (5a)$$

$$T_1(R,t) = T_v(t) \quad (5b)$$

$$T_1(S,t) = T_2(S,t) \quad (5c)$$

$$k_1\left.\frac{\partial T_1}{\partial r}\right|_{S,t} = k_2\left.\frac{\partial T_2}{\partial r}\right|_{S,t} \quad (5d)$$

$$T_2(\infty,t) = T_0 \quad (5e)$$

$$R(0) = R_0 \quad (5f)$$

$$\dot{R}(0) = 0 \quad (5g)$$

and the interface heat balance around the bubble yields

$$k_1\left.\frac{\partial T_1}{\partial r}\right|_{R,t} = \rho_v h_{fg}\dot{R}. \quad (6)$$

The initial conditions, T_0 and R_0, are the limit of superheat and initial unstable bubble radius, respectively, both defined by the critical nucleus state for homogeneous nucleation. These quantities are intrinsic properties of liquid 1 and are a function of ambient pressure for a given nucleation rate.

Since there is no mass transfer across the liquid 1/liquid 2 boundary, the purely radial velocity in this problem is continuous there. This velocity is determined by integrating eq. (1) in the two domains of liquids 1 and 2 and applying an overall mass balance around the bubble. The result is

$$v_i = \varepsilon\frac{R^2}{r^2}\dot{R}, \quad (7)$$

which is the same as for bubble growth in an infinite medium [9].

The appropriate "Rayleigh" equation for this problem is obtained by integrating eq. (2) over r twice: from R to S and again from S to ∞,

$$\int_R^\beta\left[\frac{\partial v_i}{\partial t} + v_i\frac{\partial v_i}{\partial r} = -\frac{1}{\rho_i}\frac{\partial P_i}{\partial r} + \nu_i\left(\frac{1}{r^2}\frac{\partial}{\partial r}\left(r^2\frac{\partial v_i}{\partial r}\right) - \frac{2v_i}{r^2}\right)\right]dr \quad (8)$$

where $\beta = S$ or ∞. For $r = R$,

$$P_v - P_{R1} = \frac{2\sigma_1}{R} - 2\mu_1\left.\frac{\partial v_1}{\partial r}\right|_{r=R} \quad (9)$$

(continuity) (1)

(momentum) (2)

(energy) (3)

(phase equilibrium) (4)

and for $r = S$,

$$P_{S1} - P_{S2} = \frac{2\sigma_{12}}{S} - 2(\mu_2 - \mu_1)\left.\frac{\partial v_1}{\partial r}\right|_{r=S}. \quad (10)$$

Combining eqs (7) and (8), integrating twice as indicated, and substituting eqs (9) and (10) yields the equation of motion for a spherical bubble growing from the centre of a spherical droplet:

$$[R\ddot{R} + 2\dot{R}^2]\left(1 - \bar{\varepsilon}\frac{R}{S}\right) - \varepsilon\frac{\dot{R}^2}{2}\left(1 - \bar{\varepsilon}\frac{R^4}{S^4}\right) + 4\nu_1\frac{\dot{R}}{R}\left(1 - \bar{\mu}\frac{R^3}{S^3}\right) = \frac{P_v - P_0}{\rho_1\varepsilon} - \frac{2\sigma_1}{\varepsilon\rho_1 R}\left[1 + \frac{\sigma_{12}}{\sigma_1}\frac{R}{S}\right] \quad (11)$$

where $\bar{\varepsilon} \equiv 1 - \rho_2/\rho_1$ and $\bar{\mu} \equiv 1 - \mu_2/\mu_1$.

When $S \to \infty$, or in the early stages of growth when $R \ll S$ ($R_0 \sim 10^{-7}$ cm, $S_0 \sim 1$ mm and $\sigma_1 > \sigma_{12}$), eq. (11) becomes identical to the classical Rayleigh equation for bubble growth in a superheated liquid of infinite extent. At later times, effects of the finite extent of liquid 1 reside in $\bar{\varepsilon}$, $\bar{\mu}$ and σ_{12}. Even for liquids 1 and 2 of the same properties ($\bar{\mu} = \bar{\varepsilon} = 0$) the finite mass of the droplet will effect the temporal variation of bubble radius through the term involving σ_{12} (if a surfactant is

present, though, $\sigma_{12} \to 0$). The time domain during which $P_v \to P_0$ is, however, usually small compared to the total growth time (cf. Section 4).

Neither an analytical solution to the coupled set of eqs (3)–(7), (11) nor a similarity variable exists for this set of equations and boundary conditions. Numerical methods must therefore be used.

3. METHOD OF SOLUTION

The main difficulty in obtaining a numerical solution resides in the existence of two moving boundaries: at the vapour/liquid 1 and liquid 1/liquid 2 interfaces. A coordinate transformation which immobilizes these boundaries—the so-called Landau immobilization—was used to simplify the determination of the locations of these boundaries. This transformation is illustrated in Fig. 3 and expressed as

$$\eta = \frac{r - R(t)}{S(t) - R(t)}; \quad \tau = t. \tag{12}$$

This transformation was first used by Duda *et al.* [12] in connection with analysing the growth of a single vapour bubble in an unbounded liquid (in which there is only one moving boundary), later generalized by Saitoh [13], and subsequently used in connection with a variety of melting and freezing problems [14].

The following nondimensional quantities are now introduced:

$$\bar{r} = \frac{r}{S_0} \qquad \bar{R} = \frac{R}{S_0} \qquad \bar{T} = \frac{T - T_s}{T_0 - T_s}$$

$$\tau = \frac{t\alpha_1}{S_0^2} \qquad \gamma = \frac{\alpha_2}{\alpha_1} \qquad \zeta = \frac{k_2}{k_1}$$

$$\bar{\sigma}_1 = \frac{2\sigma_1 S_0}{\alpha_1^2 \rho_1 \varepsilon} \qquad \bar{\sigma}_{12} = \frac{2\sigma_{12} S_0}{\alpha_1^2 \rho_1 \varepsilon} \qquad \xi = \frac{4\nu_1}{\alpha_1} \tag{13}$$

and $$a_p = \frac{S_0^2}{\alpha_1 \rho_1 \varepsilon}[P_v(T_0) - P_0] \qquad Ja = \frac{\rho_1 C_{p1}(T_0 - T_s)}{\rho_v h_{fg}} \qquad \bar{P} = \frac{P_v(T_v) - P_0}{P_v(T_0) - P_0}$$

where Ja is the Jakob number of liquid 1. It is a unique function of pressure through the coupling of T_s, T_0 and P_0 at the superheat limit. As $P_0 \to P_c$, $T_0 \to T_s$ and $Ja \to 0$ (see Fig. 4). A thin thermal boundary layer assumption is then clearly inaccurate for a droplet at its superheat limit at high pressures.

Introducing eqs (12) and (13) into eqs (3)–(6) yields the transformed energy equations:

$$A_i(\eta, \tau)\frac{\partial \bar{T}_i}{\partial \tau} + C_i(\eta, \tau)\frac{\partial \bar{T}_i}{\partial \eta} = \frac{\partial}{\partial \eta}\left[B_i(\eta, \tau)\frac{\partial \bar{T}_i}{\partial \eta}\right] \tag{14}$$

with

$$A_i(\eta, \tau) = \bar{r}^2(\bar{S} - \bar{R})/d_i \tag{15a}$$

$$B_i(\eta, \tau) = \bar{r}^2/(\bar{S} - \bar{R}) \tag{15b}$$

and

$$C_i(\eta, \tau) = \left[\varepsilon\bar{R}^2 + \frac{\bar{r}^3(\bar{S}^2 - \varepsilon\bar{R}^2) - \bar{r}^2}{\bar{S}^2(\bar{S} - \bar{R})^2}\right]\dot{\bar{R}}/d_i \tag{15c}$$

where $i = 1, 2$ and

$$d_1 = 1 \quad (0 < \eta < 1) \tag{16a}$$

$$d_2 = \gamma \quad (1 < \eta < \infty) \tag{16b}$$

and

$$\bar{r} = \eta(\bar{S} - \bar{R}) + \bar{R}. \tag{17}$$

The transformed initial and boundary conditions are

$$\bar{T}_1(\eta, 0) = \bar{T}_2(\eta, 0) = 1 \tag{18a}$$

$$\bar{T}_1(0, \tau) = \bar{T}_v(\tau) \tag{18b}$$

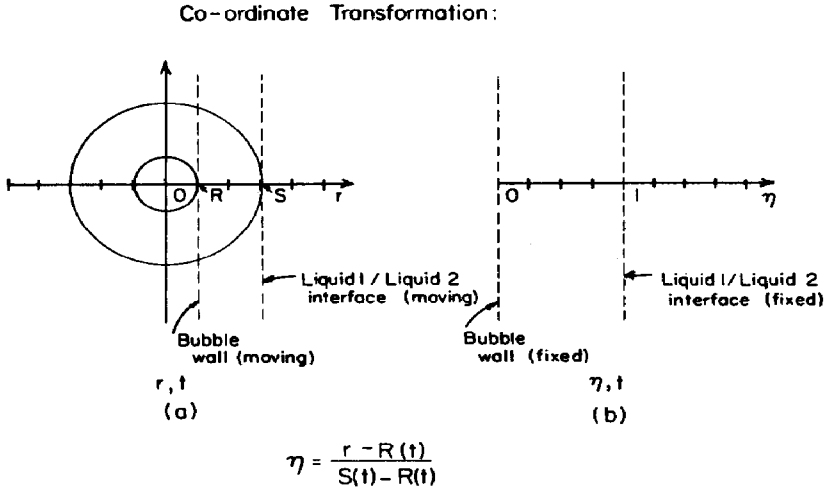

Fig. 3. Coordinate transformation to immobilize moving boundaries in a bubble/droplet system.

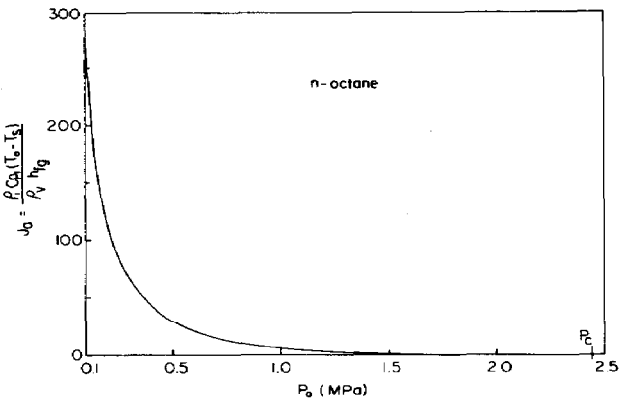

Fig. 4. Variation of Jakob number with ambient pressure for *n*-octane at its superheat limit.

$$\bar{T}_1(1,\tau) = \bar{T}_2(1,\tau) \tag{18c}$$

$$\left.\frac{\partial \bar{T}_1}{\partial \eta}\right|_{\eta=1} = \zeta \left.\frac{\partial \bar{T}_2}{\partial \eta}\right|_{\eta=1} \tag{18d}$$

$$\bar{T}_2(\infty,\tau) = 1. \tag{18e}$$

The interface heat balance [eq. (6)] is

$$\dot{\bar{R}} = \frac{Ja}{(\bar{S}-\bar{R})} \left.\frac{\partial \bar{T}_1}{\partial \eta}\right|_{\eta=0}. \tag{19}$$

Finally, the transformed momentum equation [eq. (11)] is

$$\left[\ddot{\bar{R}}\bar{R} + 2\dot{\bar{R}}^2\right]\left[1 - \bar{\varepsilon}\frac{\bar{R}}{\bar{S}}\right] - \frac{\varepsilon \dot{\bar{R}}^2}{2}\left[1 - \bar{\varepsilon}\frac{\bar{R}^4}{\bar{S}^4}\right] + \xi\frac{\dot{\bar{R}}}{\bar{R}}\left[1 - \bar{\mu}\frac{\bar{R}^3}{\bar{S}^3}\right] = a_p\bar{P} - \frac{\bar{\sigma}_1}{\bar{R}}\left[1 + \frac{\bar{\sigma}_{12}}{\bar{\sigma}_1}\frac{\bar{R}}{\bar{S}}\right]. \tag{20}$$

Equations (14)–(20) complete the formulation of the problem. No assumptions regarding the thickness of the thermal boundary layer, or neglect of thermal resistance within the droplet, have been made.

A finite difference technique was used to solve eqs (14)–(20) for $\bar{T}_1(\eta,\tau)$, $\bar{T}_2(\eta,\tau)$, $\bar{T}_v(\tau)$, $\bar{P}_v(\tau)$ and $\bar{R}(\tau)$, with a simple mass balance around the droplet relating $\bar{S}$ to $\bar{R}$ as

$$\bar{S} = [1 + \varepsilon\bar{R}^3]^{1/3}. \tag{21}$$

The Crank–Nicholson method was used to integrate the energy equation at each time step, with second-order accurate central differences used to discretize eq. (14) [15]. The momentum equation—eq. (20)—was solved using a fifth-order Runge–Kutta method.

To get the computations started, $\bar{R}$ was artificially increased by a factor of 10^{-4}–10^{-5}. Then at each time step n the following procedure was used. First the momentum equation was integrated to obtain $\bar{R}^{n+1}$ and $\dot{\bar{R}}^{n+1}$. The coefficients in the energy equation—A_i, B_i and C_i—were calculated and the set of discretized energy equations was solved simultaneously to yield a first approximation to the temperature field at time level $n+1$. The discretized form of eq. (19) was used to determine $\bar{T}_v$ at $n+1$, and the discretized energy equation again solved to get an improved value for the temperature field. This iterative process was repeated at each time step until all successively determined values of temperature at the nodal locations were within the specified accuracy. The calculations were advanced in time until liquid 1 completely evaporated at which time

$$\bar{R} \to \bar{S} = (1-\varepsilon)^{-1/3}. \tag{22}$$

Further details of the numerical scheme, including a discussion of stability, convergence and accuracy, are described elsewhere [16].

4. RESULTS AND DISCUSSION

4.1. *Introduction*

Five independent nondimensional groups control the evolution of bubble and droplet radii: Ja, $\bar{\varepsilon}$, $\bar{\mu}$, γ and ζ. Results presented encompass properties typical of hydrocarbon (liquid 1)/glycerine (liquid 2) and hydrocarbon/water combinations. $\bar{\mu}$ and $\bar{\varepsilon}$ were fixed at values typical of *n*-alkane/glycerine combinations, and the other parameters were varied to show the form of the solution.

The solution may be broadly divided into two regions: (1) a period during which the thermal boundary layer resides in liquid 1 and growth is similar to growth in an infinite medium, and (2) a later stage of growth characterized by thermal boundary layer penetration into liquid 2.

4.2. *Early stages of growth*

In the early stages several aspects of bubble growth in a droplet are very similar to growth in an infinite medium. This is illustrated in Fig. 5, which shows the evolution of P_v, T_v and $\bar{R}$ for a bubble growing in an *n*-octane droplet in glycerine at $Ja = 10$. The initial state of the droplet—T_0 and $P_0(T_0)$—corresponds to the homogeneous nucleation limit (for a nucleation rate of 10^5 nuclei/cm$^3 \cdot$ s), and the asymptotic temperatures and pressures correspond to saturation conditions. The results shown in Fig. 5 exhibit a form similar to bubble growth in an infinite medium (because the thermal boundary layer is still deep within liquid 1 for times shown in Fig. 5).

The temperature field within the droplet during this early period is shown in Fig. 6(a) for the special case $Ja = 10$. The evolution of both the thermal boundary layer (δ where $\bar{T} \to 1$) and vapour temperature $\bar{T}(\eta = 0)$ is indicated. For $\tau > 5 \times 10^{-8}$, $\bar{T}(\eta = 0) \to 0$ and the analysis becomes a purely thermal problem; the thermal boundary layer is still close to the bubble wall [$\bar{\delta} \sim 10^{-4}(\bar{S} - \bar{R})$]. The bubble is also still quite small at this time (cf. Fig. 5) and the liquid 1/liquid 2 interface has hardly expanded.

4.3. *Later stages of growth*

Eventually the thermal boundary layer extends into liquid 2 before liquid 1 completely evaporates and the energy equation for liquid 2, and associated matching conditions at the interface [eqs (18)], must be included

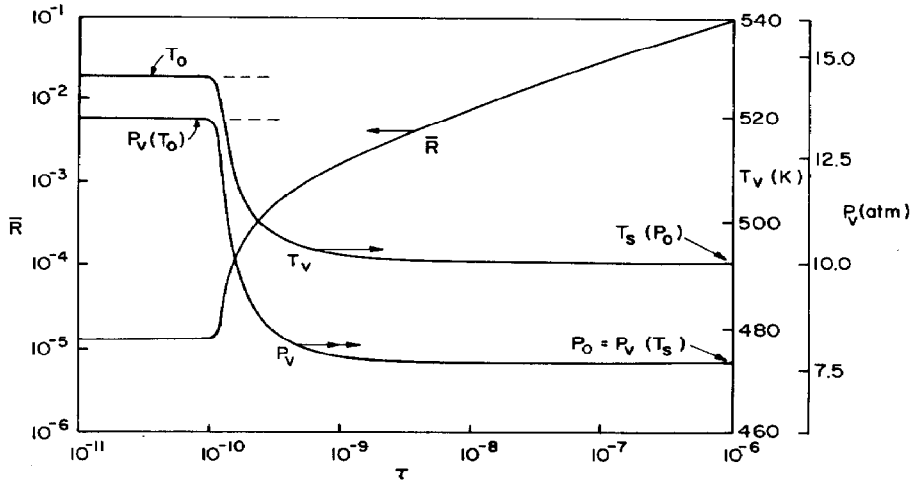

Fig. 5. Early time variation of vapour pressure, vapour temperature and radius of a bubble growing in a superheated *n*-octane droplet. Initial conditions correspond to the kinetic limit of superheat of octane at the indicated pressure: $Ja = 10$, $\gamma = 1$, $\zeta = 5$, $\varepsilon = 0.96$, $\bar{\varepsilon} = -1.2$.

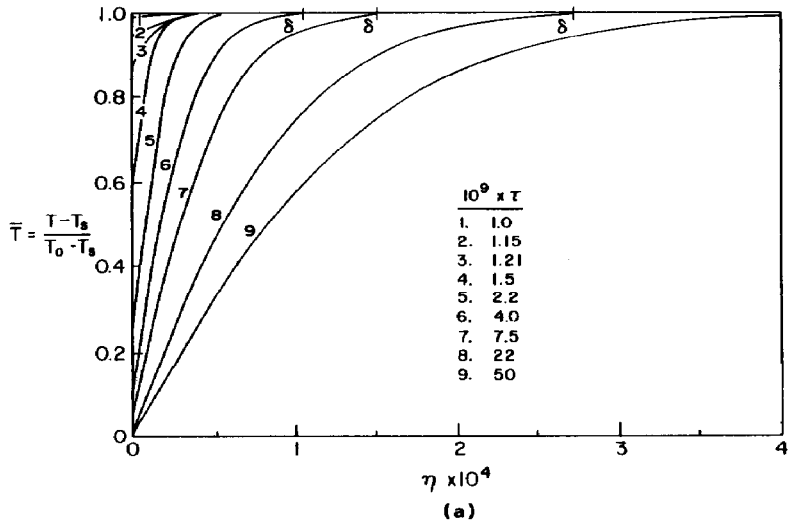

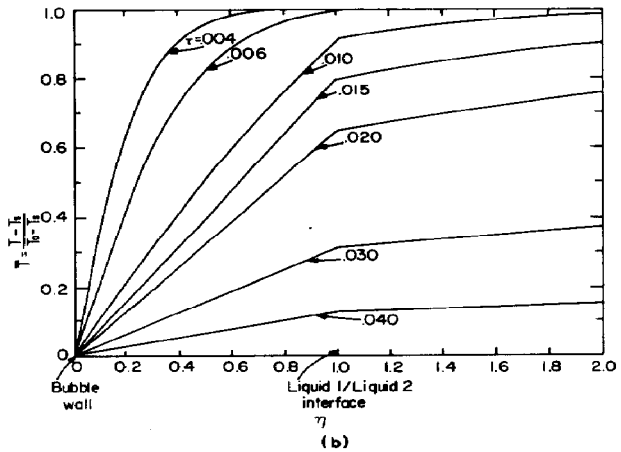

Fig. 6. Variation of temperature with position in a droplet. (a) Early times such that thermal boundary layer (δ) is still within the droplet and vapour temperature is changing with time ($\bar{T} > 0$ at $\eta = 0$) ($Ja = 10$, $\varepsilon = 0.96$, $\zeta = 5$ and $\gamma = 1$); (b) later times indicating boundary layer penetration into liquid 2.

in the analysis. Figure 6(b) illustrates the temperature field at various times during this later stage for $Ja = 10$, $\zeta = 5$ and $\gamma = 1$. For $\tau > 0.006$ the thermal boundary layer extends into liquid 2 and the temperature field is shown to become linear quickly. This is caused by rapid thinning of the liquid film of thickness $(\bar{S} - \bar{R})$ surrounding the bubble.

The effect of thermal boundary layer penetration in liquid 2 on bubble growth rate is shown in Fig. 7(a) and (b) for the indicated ranges of Ja, γ and ζ. As expected, growth is independent of liquid 2 properties during the period in which the thermal boundary layer resides in liquid 1. However, when penetration into liquid 2 does occur, the bubble (and droplet) growth rate can undergo rather dramatic changes, depending on the relative values of ζ and γ. For $\zeta > 1$, a less steep temperature gradient exists in liquid 2 than in liquid 1. This in turn creates a gradient in liquid 1 at $\eta = 1$ larger than would be realized if $\zeta = 1$ (i.e. when the properties of liquids 1 and 2 are identical). This increased temperature gradient at $\eta = 1$ translates into a larger temperature gradient at $\eta = 0$ (the bubble wall). The bubble then should experience an increase in its growth rate. The opposite is true when $\zeta < 1$. This behaviour cannot be predicted from an analysis which (1) neglects the thermal resistance of liquid 1, and/or (2) assumes results from growth in an infinite medium apply to this problem.

Similar results occur when γ varies while ζ is fixed. This is shown in Fig. 7(b) for $Ja = 10$. The bubble grows progressively faster as γ decreases. For example, a lowering of γ (for $\zeta = 1$) when $\rho_1 C_{p1}$ is fixed (liquid 2 is changed) means that the heat capacity per unit volume of liquid 2, $\rho_2 C_{p2}$, is progressively increased. The ability of liquid 2 to supply more heat to liquid 1 then increases as γ decreases, and the growth rate correspondingly increases when the thermal boundary layer enters liquid 2.

The very early period of growth wherein the pressure field is still changing is undetectable on the scale of Fig. 7. The region around the origin in Fig. 7 is shown on an expanded scale in Fig. 5. For the time scales in Fig. 7, $P \simeq P_0$ and $\bar{T}(\eta = 0) \simeq 0$, though there will always (at least numerically) be a nonzero difference in pressure across the evaporating boundary. The effect of this small pressure difference on growth rate is negligible for conditions of the calculations appearing in Fig. 7.

As liquid 1 evaporates, both the internal vapour bubble and the droplet as a whole expand. Figure 8 illustrates a typical evolution of $\bar{S}$ and $\bar{R}$ for $Ja = 50$ for one representative set of conditions. When $\bar{R} \to \bar{S}$, the droplet is completely vapourized. It is worth noting that the droplet is nearly completely taken up by vapour with just a thin layer of liquid 1 around it $(\bar{S} - \bar{R})$ when $\tau > 2 \times 10^{-4}$ for conditions of the calculations shown in Fig. 8.

As the Jakob number increases, the time at which liquid 2 effects growth (i.e. when $\bar{\delta} > \bar{S} - \bar{R}$) increases and the characteristic "fanning" of the growth curves shown in Fig. 7 originates at progressively larger times. For sufficiently high Jakob number, the thermal boundary layer remains within liquid 1 throughout nearly the entire period of growth, except when $\bar{S} \to \bar{R}$ at which time the boundary layer must of course contact the liquid 1/liquid 2 boundary. Growth is then independent of liquid 2 properties and resembles

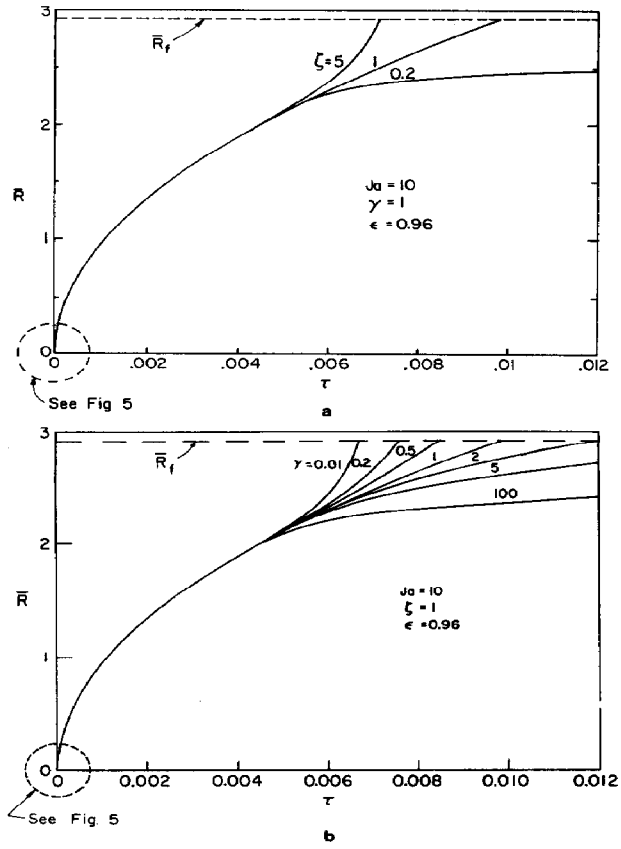

Fig. 7. Later evolution of bubble radius ($\bar{R}$) with time (τ). (a) Effect of ζ for $\gamma = 1$ (properties of *n*-octane at its superheat limit at 1.2 MPA); (b) effect of γ for $\zeta = 1$. Fanning of curves signify boundary layer penetration into liquid 2.

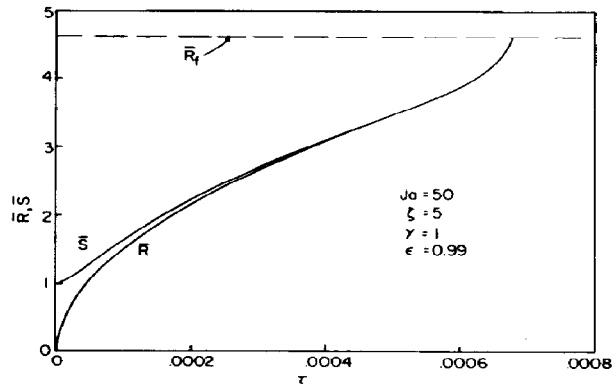

Fig. 8. Evolution of both bubble ($\bar{R}$) and droplet ($\bar{S}$) radii for $Ja = 50$, $\zeta = 5.0$ and $\gamma = 1$. Curves terminate when $\bar{R} \to \bar{S} = \bar{R}_f$ and the droplet is completely evaporated.

growth in an infinite medium. Figure 9 illustrates this for $Ja = 100$. At this high Jakob number, $\bar{T}(\eta = 0) \to 0$ at times much shorter than indicated in this figure.

Two factors affect the bubble and droplet expansion rate: (1) the pressure difference $\Delta P = P_v - P_0$ through the equation of motion, and (2) the temperature difference $\Delta T = T_0 - T_v$ as it determines the heat transfer rate to the bubble. The initial values of these "driving forces" are directly related to P_0 through the nucleation rate, but their subsequent evolution as shown in Fig. 10 for the octane/glycerine system is governed by the dynamics and thermal analysis presented here (the thermal boundary layer resided in liquid 1 for time scales indicated in Fig. 10). Variations in Ja are in effect variations in P_0 (Fig. 4). As P_0 increases (Ja decreases) the initial ΔT and ΔP, defined by the superheat limit, both decrease as shown in Fig. 10. A lowering in ΔT in particular has a more pronounced effect on growth rate than does a lowering in ΔP because dynamic effects are very quickly dissipated while the bubble has hardly expanded (Fig. 5). A reduction in ΔT (increase in P_0) results in a reduced growth rate (comparatively less heat supply to the bubble), and a longer time to evaporate liquid 1. This is evident by comparing the time scales in Figs 7–9. The effect of increasing P_0 noted above has been experimentally observed [8].

It is interesting to explore the similarity of purely heat transfer controlled bubble growth in a *droplet* (i.e. finite volume) to the bubble growth law characteristic of an *infinite medium*. For this purpose, we recall that the temporal variation of R for growth in an infinite medium has the form

$$R \sim t^q \tag{23}$$

where $q = 1/2$. For purposes of comparison, calculations for $Ja = 10$, $\zeta = 1$ and $\varepsilon = 0.9995$ (a hypothetical value chosen so that $\bar{S} \to \bar{R}_f$ at a time large enough to illustrate the similarity clearly) are displayed in Fig. 11 on a logarithmic scale for three values of γ. For $\tau < 1.1 \times 10^{-2}$ in Fig. 11 $q = 1/2$ regardless of liquid 2 properties. Growth is then identical to a bubble in an infinite medium of liquid 1 because the boundary layer is still within the droplet during this period. For $\gamma = 1$ the indicated line is identical to the asymptotic heat transfer limit (e.g. [9]) regardless of placement of the thermal boundary layer. On the other hand, for general γ and $\tau \gtrsim 1.1 \times 10^{-2}$ in Fig. 11 the thermal boundary layer extends into liquid 2. q may then be larger or smaller than 1/2. When $\gamma > 1$, the temperature gradient in liquid 2 is larger than the corresponding gradient in liquid 1. The growth rate decreases compared to the infinite medium case and $q < 1/2$. The opposite is true when $\gamma < 1$. Eventually as $\delta \gg S - R$, the thermal resistance of liquid 1 becomes of negligible importance, and the temperature field resembles that which would exist for a bubble growing in an infinite medium of liquid 2, though ρ_v and h_{fg} would correspond to liquid 1; again, $q \to 1/2$. In general, q will be a function of the depth of penetration of the thermal boundary layer into liquid 2.

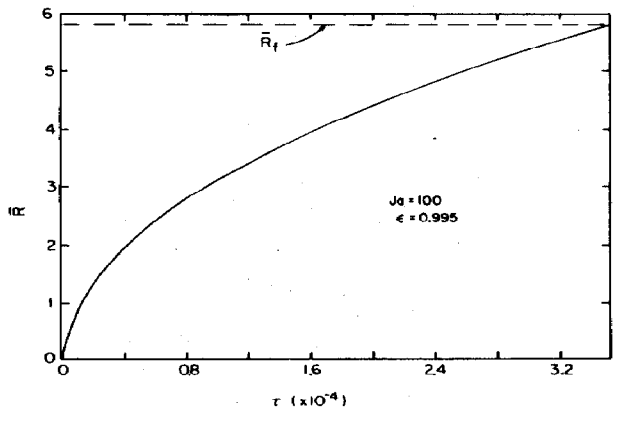

Fig. 9. Evolution of bubble radius within a droplet when the thermal boundary layer resides within the droplet throughout its entire evaporation. $Ja = 100$ and $\varepsilon = 0.995$.

4.4. *Comparison with experiment*

The model developed here applies under non-explosive, initially isothermal, conditions such that the evaporating boundary is smooth, the bubble does not oscillate and there is no relative velocity between droplet and ambient. No studies have been reported which conform to these conditions in all respects. In particular, most previous studies employed slowly moving droplets. In view of the small thermal diffusivity of most liquids—$\alpha \simeq 10^{-3}$–10^{-4} cm^2/s—the Péclet number can still be quite large even for slowly moving droplets ($U_\infty \sim 1$ cm/s). Values have ranged from about 10 to over 10^4. Only the experiments performed by Apfel and Harbison [11] corresponded to $Pe = 0$. But the conditions of their experiments were such that vaporization was explosive, the droplets oscillated and they had an ill-defined shape during evaporation. Another experimental method [8] involving suspended droplets at their superheat limits could reach conditions such that evaporation was slow enough that droplet oscillations were never observed (i.e. pressures above atmospheric). However, the droplets were slowly moving and in particular $Pe \sim 100$, so the application of the present analysis to data obtained from this method must be discussed further.

During the period in which the thermal boundary layer resides in the droplet, the present analysis can still be applied even for a droplet which is moving. This is because conditions outside the droplet will not effect growth when the boundary layer resides in the droplet (cf. Fig. 7). Deviations between measured droplet radii and values predicted from the present analysis might be expected only after boundary layer penetration in liquid 2 because then the energy equation for liquid 2 enters the analysis. This equation must contain additional contributions (of order Pe/Ja^3) in the convective terms to account for translational motion of liquid 2 (e.g. [2]), while the energy equation of liquid 1 is unaltered (assuming that this slow external movement does not induce circulatory motion in liquid 1, which we neglect in view of the relative thinness of the

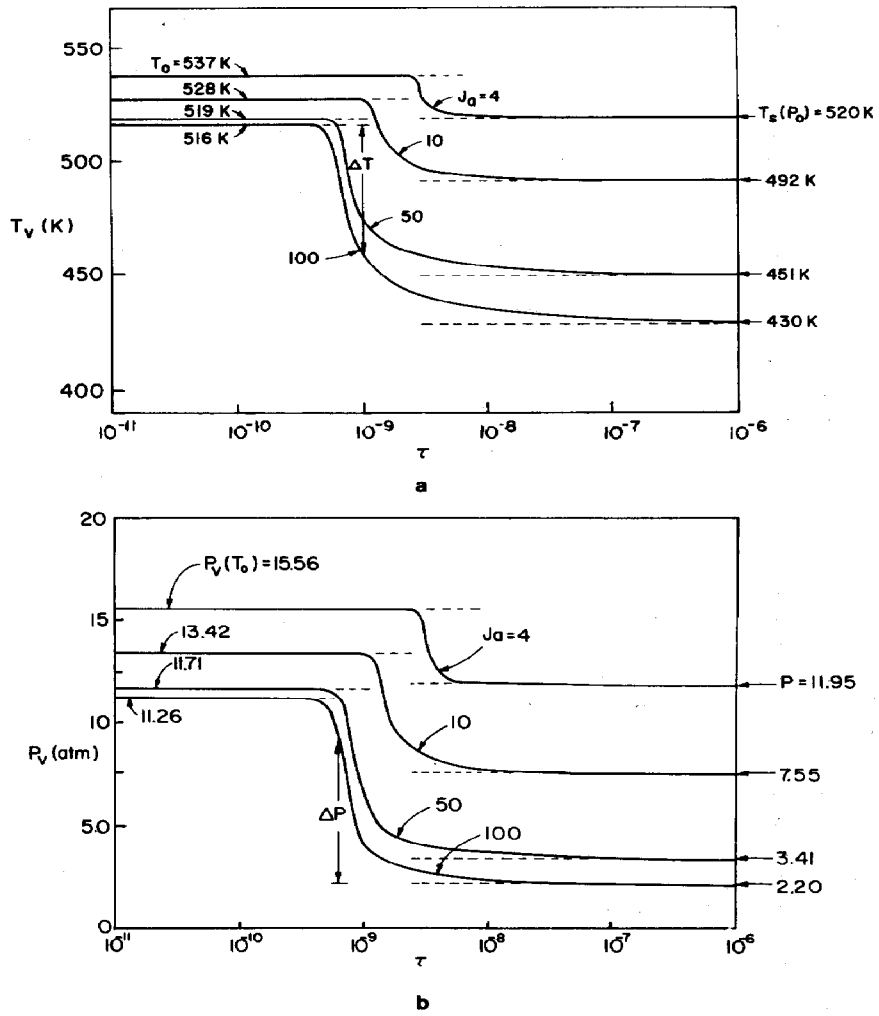

Fig. 10. Effect of Jakob number on evolution of vapour pressure, P_v, and vapour temperature, T_v, within a bubble growing in an *n*-octane droplet suspended in glycerine. Large time asymptotes correspond to saturation temperature (a) and pressure (b) at ambient pressure P_0 (b). Initial conditions (small time asymptotes) are limit of superheat at P_0 (a) and vapour pressure within critical size nucleus (b). ΔT and ΔP indicate temperature (a) and pressure (b) driving forces for bubble growth.

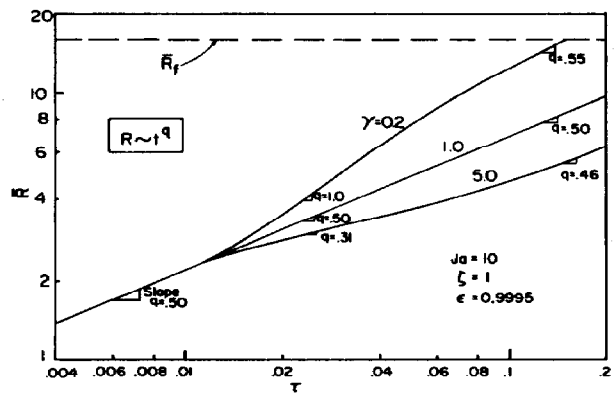

Fig. 11. Effect of time (τ) on bubble growth exponent [eq. (23)] for heat transfer controlled growth of a bubble in a droplet at various γ, and $\zeta = 1$, $\varepsilon = 0.9995$ (a hypothetical value). Thermal boundary layer penetrates into liquid 2 at $\tau > 0.011$.

liquid 1 layer around the internal bubble as previously discussed). The momentum equation is also altered by external motion, but its effect on the temperature field will be felt only during the very early period of growth during which the pressure within the bubble drops to its saturation value. During this period the radius characteristically hardly changes so the effect of droplet translation on the temporal variation of radius through the momentum equation is negligible. As a result, measurements obtained using the floating droplet technique [8] were compared with the present calculations. The method was modified to provide a chamber with flat glass sides so as to eliminate distortion due to curvature. Only $\bar{S}$ (overall droplet radius) was measured, as the experimental method did not allow an unambiguous determination of $\bar{R}$.

Figure 12 compares predicted and measured droplet radii. Experimental conditions were such that $S_0 \simeq 0.06$ cm, $Ja = 4$, $\varepsilon = 0.91$ and $Pe = 145$ with *n*-

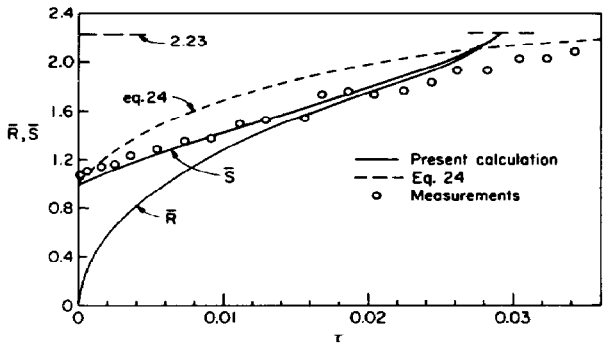

Fig. 12. Comparison between calculated droplet radii and values measured using the apparatus of Ref. 8 for an *n*-octane droplet boiling in glycerine at $Ja = 4$, $\varepsilon = 0.91$, $\gamma = 1.67$, $\zeta = 4.1$ and $Pe = 145$. The dotted line is a quasi-steady solution [1, 2] from eq. (24).

octane as the droplet (liquid 1) and glycerine liquid 2. Vaporization at these conditions was non-explosive, though the *n*-octane droplet was still at its superheat limit. The time for development of a steady vapour temperature and pressure was sufficiently small on the scale of Fig. 12 to be undetectable. The agreement is reasonable for the period in which the thermal boundary layer resides in the droplet. When $\tau > 0.02$ the boundary layer extends into liquid 2 and the energy equation for liquid 2 enters the analysis.

An analytical solution for boiling of a droplet in another immiscible liquid was presented by Sideman and co-workers [1, 2] for the extreme assumptions of: (1) no radial convection, (2) constant and uniform temperature in liquid 1, (3) quasi-steady heat transfer in liquid 2 such that the temperature field adjusts instantaneously to changes in droplet radius, (4) inviscid and uniform translatory motion of liquid 2 around the liquid 1 droplet and (5) partial heat supply to the bubble in a spherical droplet. Heat transfer was assumed to be entirely by conduction and translational convection in their analysis. These assumptions are inappropriate during the early period of growth when the boundary layer resides in liquid 1 and the temperature field is transient. It is a better approach after boundary layer penetration in liquid 2 when translational convection may be important (for a moving droplet) and the quasi-steady approximation may be more reasonable. In variables defined here, their solution is the following:

$$\bar{S} = (1-\varepsilon)^{-1/3}\left\{1-\varepsilon\left[\left(\frac{9}{2\pi}\right)^{1/2} \times (1-\varepsilon)\,Ja\,Pe^{1/2}\tau - 1\right]^2\right\}^{1/3}. \quad (24)$$

Equation (24) was developed for a geometry consisting of a puddle of liquid at the bottom of a droplet with a planar liquid/vapour interface. Figure 12 compares droplet radii ($\bar{S}$) predicted by eq. (24) (dotted line) with the present solution. The over-prediction of eq. (24) during the period in which the boundary layer resides in liquid 1 is due to the quasi-steady assumption and the neglect of heat transfer in the droplet. The present analysis accounts for the temporal variation of the temperature field in liquid 1 which results in a slower growth during this early period.

Additional experiments are needed to conform more closely to the conditions of the present analysis. These experiments should employ levitated droplets at high pressure to reach truly isothermal conditions and improved photographic methods to increase the accuracy of the measurements. Work is continuing along these lines. Finally, the present solution may be useful as a basis for comparison with future treatments of this problem, similar to the value full solutions to the governing equations for bubble growth in infinite media [17, 18] have had as a test of the value of corresponding approximate treatments [19, 20].

5. CONCLUSIONS

Bubble growth in an isolated initially isothermal liquid droplet at its superheat limit in another immiscible liquid was analysed by solving the full set of coupled momentum and energy equations for the droplet and ambient liquid. For sufficiently different properties of liquids 1 and 2, the bubble growth rate within liquid 1 can be increased or decreased. During an early period of growth, or for large Jakob numbers, the thermal boundary layer resides entirely within the droplet and growth is nearly identical to bubble growth in an infinite medium. Only when the thermal boundary layer penetrates into liquid 2 do the properties of liquid 2 effect growth. Qualitative agreement of the present model with experiments involving slowly moving droplets exists for the period in which the boundary layer resides in the drop. There exists a need for more experiments to resolve precisely the effects of penetration of the thermal boundary layer into liquid 2.

Acknowledgements—This work was supported by NSF grant No. CPE-8106348 from the Thermodynamics and Transport Phenomena program (Dr. Robert M. Wellek, Program Director) and by the Department of Energy, Office of Basic Energy Sciences—Division of Engineering and Mathematical Sciences (Dr. Oscar P. Manley, Project Monitor) under contract No. DE-AC02-83ER13092. This support has been gratefully appreciated.

NOTATION

h_{fg}	heat of vaporization of liquid 1
Ja	Jakob number [eq. (13)]
k_i	thermal conductivity of liquid i ($i = 1, 2$)
Pe	Péclet number ($= U_\infty S_0/\alpha_2$, where U_∞ is a characteristic free stream velocity)
P_i	pressure within liquid i
P_0	pressure at infinity in liquid 2
P_{R1}	pressure within liquid 1 at $r = R$
P_{S1}	pressure within liquid 1 at $r = S$
P_{S2}	pressure within liquid 2 at $r = S$
P_v	equilibrium vapour pressure of liquid 1
r	radial position

R bubble radius
R_0 initial bubble (or critical nucleus) radius
$\dot{R}$ velocity of bubble wall
S droplet radius
S_0 initial liquid droplet radius
t time
T_i temperature within liquid i
T_0 homogeneous nucleation limit of liquid 1 at P_0
T_s saturation temperature of liquid 1 at P_0
T_v vapour temperature within bubble
v_i radial velocity in liquid i

Greek letters

α_i thermal diffusivity of liquid i
γ $= \alpha_2/\alpha_1$
ε density ratio $(= 1 - \rho_v/\rho_1)$
$\bar{\varepsilon}$ density ratio $(= 1 - \rho_2/\rho_1)$
ζ conductivity ratio $(= k_2/k_1)$
ρ_v density of vapour i
ρ_i density of liquid i
σ_1 surface tension of liquid 1
σ_{12} liquid 1/liquid 2 interfacial tension
ν_1 kinematic viscosity of liquid 1
μ_i viscosity of liquid i
$\bar{\mu}$ viscosity ratio $(= 1 - \mu_2/\mu_1)$

REFERENCES

[1] Sideman S. and Isenberg J., *Desalination* 1967 **2** 207.
[2] Sideman S. and Taitel Y., *Int. J. Heat Mass Transfer* 1964 **7** 1273.
[3] Tochitani Y., Nakagawa T., Mori Y. H. and Komotori K., *Wärme-und Stoffubertragung* 1977 **10** 71.
[4] Selecki A. and Gradon L., *Int. J. Heat Mass Transfer* 1976 **19** 925.
[5] Mokhtarzadeh M. R. and El-Shirbini A. A., *Int. J. Heat Mass Transfer* 1979 **22** 27.
[6] Gradon L. and Selecki A., *Int. J. Heat Mass Transfer* 1977 **20** 459.
[7] Lasheras J. C., Yap L. T. and Dryer F. L., Fall Western States Section Meeting, Combustion Institute, Paper No. WSCI82-94, 1982.
[8] Avedisian C. T., *J. Heat Transfer* 1982 **104** 750.
[9] Scriven L. E., *Chem. Engng Sci.* 1959 **10** 1.
[10] Shepherd J. E. and Sturtevant B., *J. Fluid Mech.* 1982 **121** 379.
[11] Apfel R. E. and Harbison J. P., *J. Acoust. Soc. Am.* 1975 **57**(6), 1371.
[12] Duda J. J., Malone M. F., Notter R. H. and Vrentas J. S., *Int. J. Heat Mass Transfer* 1975 **18** 901.
[13] Saitoh T., *J. Heat Transfer* 1978 **100** 294.
[14] Prusa J. and Yao L. S., 21st ASME/A.I.Ch.E. National Heat Transfer Conference, Seattle, Paper No. 83-HT-18, 24–28 July 1983.
[15] Babuska T., Prager M. and Vitasek E., *Numerical Processes in Differential Equations* SNIL, Prague 1966.
[16] Suresh K., M.S. Thesis, Dept. of Mech. and Aero. Eng., Cornell University, Ithaca, NY 1984.
[17] Dalle-Donne M. and Ferranti M. P., *Int. J. Heat Mass Transfer* 1975 **18** 901.
[18] Saitoh T. and Shima A., *J. mech. Engng Sci.* 1977 **19**(3) 101.
[19] Prosperetti A. and Plesset M., *J. Fluid Mech.* 1978 **85**(2) 349.
[20] Mikic B. B., Rohsenow W. M. and Griffith P., *Int. J. Heat Mass Transfer* 1970 **13** 657.